

Multimodal Generative Retrieval Model with Staged Pretraining for Food Delivery on Meituan

Boyu Chen

Beijing University of Posts and Telecommunications
Beijing, China
chenbys4@bupt.edu.cn

Yuqing Li

Xingxing Wang
Meituan
Beijing, China
liyuqing16@meituan.com
wangxingxing04@meituan.com

Tai Guo

Weiyu Cui
Meituan
Beijing, China
guotai02@meituan.com
cuiweiyu02@meituan.com

Chuan Shi

Cheng Yang*
Beijing University of Posts and Telecommunications
Beijing, China
shichuan@bupt.edu.cn
yangcheng@bupt.edu.cn

Abstract

Multimodal retrieval models are becoming increasingly important in scenarios such as food delivery, where rich multimodal features can meet diverse user needs and enable precise retrieval. Mainstream approaches typically employ a dual-tower architecture between queries and items, and perform joint optimization of intra-tower and inter-tower tasks. However, we observe that joint optimization often leads to certain modalities dominating the training process, while other modalities are neglected. In addition, inconsistent training speeds across modalities can easily result in the one-epoch problem. To address these challenges, we propose a staged pretraining strategy, which guides the model to focus on specialized tasks at each stage, enabling it to effectively attend to and utilize multimodal features, and allowing flexible control over the training process at each stage to avoid the one-epoch problem. Furthermore, to better utilize the semantic IDs that compress high-dimensional multimodal embeddings, we design both generative and discriminative tasks to help the model understand the associations between SIDs, queries, and item features, thereby improving overall performance. Extensive experiments on large-scale real-world Meituan data demonstrate that our method achieves improvements of 3.80%, 2.64%, and 2.17% on R@5, R@10, and R@20, and 5.10%, 4.22%, and 2.09% on N@5, N@10, and N@20 compared to mainstream baselines. Online A/B testing on the Meituan platform shows that our approach achieves a 1.12% increase in revenue and a 1.02% increase in click-through rate, validating the effectiveness and superiority of our method in practical applications.

*Corresponding author.

Permission to make digital or hard copies of all or part of this work for personal or classroom use is granted without fee provided that copies are not made or distributed for profit or commercial advantage and that copies bear this notice and the full citation on the first page. Copyrights for components of this work owned by others than the author(s) must be honored. Abstracting with credit is permitted. To copy otherwise, or republish, to post on servers or to redistribute to lists, requires prior specific permission and/or a fee. Request permissions from permissions@acm.org.

Conference'17, Washington, DC, USA

© 2026 Copyright held by the owner/author(s). Publication rights licensed to ACM.
ACM ISBN 978-x-xxxx-xxxx-x/YY/MM
<https://doi.org/10.1145/nnnnnnnn.nnnnnnn>

CCS Concepts

- Information systems → Retrieval models and ranking.

Keywords

Multimodal Retrieval, Generative Retrieval

ACM Reference Format:

Boyu Chen, Tai Guo, Weiyu Cui, Yuqing Li, Xingxing Wang, Chuan Shi, and Cheng Yang. 2026. Multimodal Generative Retrieval Model with Staged Pretraining for Food Delivery on Meituan. In . ACM, New York, NY, USA, 11 pages. <https://doi.org/10.1145/nnnnnnnn.nnnnnnn>

1 Introduction

Food delivery search has become an indispensable part of users' daily lives. Users typically submit textual queries to retrieve a set of relevant items and select desired products for purchase, making the quality of item retrieval a critical factor that directly impacts platform transaction revenue. As user needs become increasingly diverse, relying solely on textual features is no longer sufficient to address all queries. This necessity has led to the emergence of multimodal retrieval models [2, 7, 14, 17, 32, 42], which integrate and process various types of product features to enable richer and more precise retrieval results. Recent advances in large models have accelerated the development of multimodal retrieval [6, 23, 38] by enabling the extraction of high-quality feature embeddings, thus providing a strong foundation for item retrieval and matching.

The mainstream framework for multimodal retrieval models is the dual-tower architecture [1, 2, 6, 17, 23, 32, 38, 42], in which the query and item towers respectively encode their feature embeddings. Compared to unimodal retrieval models [3, 8, 12, 13, 25, 27–29], multimodal retrieval models integrate various types of features (e.g., text and images) within the item tower, and employ specialized network modules to process each modality. Moreover, multiple objectives are adopted to optimize the model. To obtain high-quality fused representations, these models typically employ contrastive learning between different modalities of the same sample to ensure consistency (e.g., image2text). Furthermore, to strengthen the

association between the two towers, additional contrastive learning tasks are designed between the query and various modality-specific or fused features from the item tower (e.g., query2image, query2text, and query2item), thereby further enhancing the model's downstream retrieval capability.

Previous multimodal retrieval models typically employ **joint optimization** of multiple objectives to improve overall performance [2, 6, 42]. However, as shown in Figure 1 (a), our analysis of the loss trajectories during joint training reveals that the reduction in query2item loss closely mirrors that of query2text loss, while losses associated with other modalities exhibit limited correlation. Furthermore, due to differences in learning difficulty across modalities, the loss for image features converges significantly more slowly than that for textual features. This imbalance can lead to the so-called one-epoch problem [9, 40], where the model overfits features that are easier to learn while under-optimizing more challenging ones, ultimately resulting in degraded overall performance. To further investigate this phenomenon, we conduct an experiment in which image embeddings are replaced with randomly generated vectors. As illustrated in Figure 1 (b), the retrieval performance remains nearly unchanged, indicating that the model tends to ignore image features.

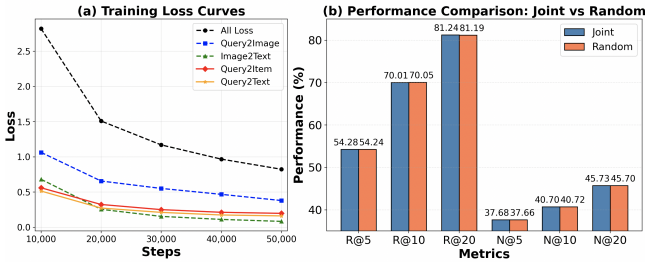


Figure 1: (a) Loss trends of different objectives during joint optimization. (b) Performance comparison between the jointly optimized model and the model with randomly generated image embeddings.

In addition, the introduction of multimodal features in online deployment environments imposes significant storage and computational burdens. To this end, generative retrieval models have emerged, employing residual quantized variational autoencoders (RQ-VAE) [19] to discretize high-dimensional embeddings into compact semantic IDs (SIDs), thereby improving retrieval efficiency and feature expressiveness. As newly generated intermediate features, SIDs lack dedicated pretraining in large language models (LLMs), resulting in limited semantic understanding and utilization. Previous methods [5, 15, 18, 26, 31, 35, 36, 41] typically employ only discriminative losses for downstream fine-tuning, which are insufficient for helping the model understand the associations between SIDs, queries, and item features.

To address these challenges, we propose SMGR, which is a **multimodal generative retrieval model with staged pretraining** for food delivery on Meituan. We employ staged pretraining to ensure that the model focuses on specific objectives at each phase, thereby alleviating the issue of other features being neglected due

to the dominance of a single modality. Also, this approach effectively avoids the one-epoch problem caused by inconsistent training speeds across modalities. After progressively optimizing high-quality multimodal representations, we leverage RQ-VAE to transform these features into multiple SIDs. Furthermore, we introduce both generative and discriminative tasks for SIDs understanding and downstream adaptation, enabling the model to effectively learn and utilize SIDs. Extensive offline experiments on large-scale real-world Meituan data demonstrate that our method achieves improvements of 3.80%, 2.64%, and 2.17% on R@5, R@10, and R@20, and 5.10%, 4.22%, and 2.09% on N@5, N@10, and N@20 compared to state-of-the-art baselines. In online A/B testing on the Meituan platform, our method also demonstrates significant improvements compared to the online baseline. The contributions of this work are as follows:

- We empirically find that, in multimodal retrieval scenarios, joint pretraining may cause the optimization process to be dominated by certain modalities, resulting in the neglect of other modality features. In addition, the joint optimization is prone to the one-epoch problem.
- We propose a staged pretraining strategy to address the above limitation. Also, to better utilize the semantic IDs that compress high-dimensional multimodal embeddings, we employ both generative and discriminative tasks to facilitate the model's understanding, ultimately enhancing overall model performance.
- Extensive offline experiments on the Meituan platform demonstrate significant improvements of our proposed method over various baselines. In addition, online A/B testing shows that, our approach achieves a 1.12% increase in revenue and a 1.02% increase in click-through rate (CTR), resulting in substantial gains.

2 Related Work

2.1 Multimodal Retrieval Model

Multimodal dual-tower models [2, 6, 14, 17, 23, 32, 38, 42] have demonstrated strong performance in complex retrieval scenarios and have become the mainstream framework for multimodal retrieval tasks. Building upon the traditional dual-tower architecture [3, 11, 21], these models extend the item tower from representing only textual features to incorporating multimodal features such as images, audio, and video. Each modality is encoded using dedicated encoders, including CNNs [11, 21, 22], RNNs, Transformers [13, 20], or ViTs [34], and the resulting representations are fused via concatenation [2], addition [17, 38], multilayer perceptron (MLP) [23], or attention mechanisms [6, 42] to produce fixed-length multimodal embeddings. During training, contrastive learning is commonly employed for both intra-tower and inter-tower optimization. Intra-tower optimization aims to align representations of the same sample across different modalities to improve feature fusion, while inter-tower optimization focuses on matching relevant query-item pairs to enhance retrieval performance. Some approaches [2, 6, 42] further design joint optimization strategies to fully exploit multimodal information.

Despite their effectiveness, multimodal dual-tower models face several practical challenges. Modalities with simpler semantics and

higher relevance to queries may dominate the optimization process, resulting in underutilization of other modality features. Inconsistent training speeds across modalities can also lead to the one-epoch problem. Additionally, these models require substantial storage and computational resources for deployment. Online inference is often constrained by efficiency, while offline indexing increases storage demands and is susceptible to semantic drift due to data distribution shifts. To maintain performance, periodic model fine-tuning is necessary, but this incurs considerable maintenance costs.

2.2 Generative Retrieval Model

Generative retrieval models [24, 30, 37, 39] have shown significant research value in addressing challenges related to storage, computation, and fine-tuning in recent years. These models leverage the RQ-VAE [19] technique from generative recommendation systems, performing residual quantization on original high-dimensional embeddings through multi-layer codebooks to discretize continuous embedding vectors into SIDs. These SIDs can be used directly as item features or as side information to enhance the recall process, thereby improving feature representation quality and retrieval efficiency.

During model training, codebook parameters are jointly optimized using reconstruction loss, codebook loss and commitment loss, enabling the encoder to learn high-quality discrete representations. Specifically, the model maps the original embeddings to positions in multi-layer codebooks, and these positions serve as low-dimensional SIDs for efficient matching and retrieval within the dual-tower architecture. This approach not only significantly reduces storage and computational resource consumption, but also enhances the adaptability of SIDs to dynamic changes in online data distributions, thereby facilitating rapid fine-tuning and efficient deployment.

Subsequent research has further explored the integration of RQ-VAE techniques into multimodal retrieval models [5, 18, 26, 31], generating SIDs not only for individual modality features but also for their fused representations. These SIDs are partially or fully utilized in downstream retrieval tasks to enhance model performance. However, the proliferation of SIDs introduces new challenges in their selection and utilization. As newly generated features, the effectiveness of multimodal SIDs rely heavily on subsequent fine-tuning, necessitating dedicated training and optimization to fully realize their potential in retrieval tasks. Moreover, efficiently leveraging SIDs during the retrieval process remains a critical issue that significantly impacts the practical performance of these models.

3 Preliminaries

In this section, we will introduce the dual-tower dense retrieval framework adopted by the Meituan food delivery retrieval system.

In this framework, each input x represents either a query or an item along with its associated attributes. For each input x , we first apply a shared LLM encoder, which processes x according to a predefined prompt template. Specifically, the input text and related attributes are concatenated and fed into the LLM, which tokenizes and encodes the input to produce a sequence of 1024-dimensional vectors. We select the last vector in this sequence (i.e., the EOS position) as the semantic representation of the entire input.

Formally, let x_q and x_i denote the input features of a query and an item, respectively. Their semantic representations are given by $e_q = \text{LLM}(x_q)$ and $e_i = \text{LLM}(x_i)$, where $e_q, e_i \in \mathbb{R}^{1024}$.

To meet the requirements of online storage and real-time retrieval, the query tower and item tower independently compress their 1024-dimensional semantic representations using separate MLP, resulting in the final semantic vectors h_q and h_i :

$$h_q = \text{MLP}_Q(e_q), \quad h_i = \text{MLP}_I(e_i), \quad (1)$$

where $h_q, h_i \in \mathbb{R}^{128}$, and MLP_Q and MLP_I denote the independent projection networks for the query and item towers, respectively.

During the retrieval phase, the system precomputes and stores the semantic vectors h_i for all candidate items $i \in \mathcal{I}$. For each incoming query q , the semantic vector h_q is computed in real time. The relevance between the query and each candidate item is then measured by a similarity function $s(h_q, h_i)$, where cosine similarity is typically used:

$$s(h_q, h_i) = \frac{h_q^\top h_i}{\|h_q\| \|h_i\|}. \quad (2)$$

To improve retrieval efficiency, the system employs FAISS [4] as the approximate nearest neighbor (ANN) search engine. FAISS enables efficient identification of the Top- K items most similar to the query vector from a large-scale item vector database. The final retrieval result for a given query q is formulated as:

$$\mathcal{I}_q = \text{Top-}K(\{i : s(h_q, h_i) \mid i \in \mathcal{I}\}). \quad (3)$$

Considering the potential semantic gap between different features, we adopt contrastive learning to reduce the distribution discrepancy and obtain high-quality semantic embeddings. The core idea of contrastive learning is to optimize the model such that the semantic representations of related samples are closer in the embedding space, while those of unrelated samples are effectively separated. Here, related samples typically refer to positive samples matching the ground truth, and unrelated samples are negative samples obtained through random sampling or other strategies. For unified reference in subsequent method sections, we define the basic contrastive learning loss as follows:

$$\mathcal{L}_{\text{InfoNCE}}(x, x^+, \{x^-\}) = -\log \frac{\exp\left(\frac{s(x, x^+)}{\tau}\right)}{\exp\left(\frac{s(x, x^+)}{\tau}\right) + \sum_{x^-} \exp\left(\frac{s(x, x^-)}{\tau}\right)}, \quad (4)$$

where x denotes the input sample, x^+ denotes the positive sample semantically related to x , $\{x^-\}$ denotes the set of negative samples unrelated to x , $s(\cdot, \cdot)$ is a similarity function (e.g., cosine similarity), and τ is a temperature coefficient that controls the sharpness of the similarity distribution.

4 Methodology

Our method consists of three principal components: staged pretraining for embedding learning, semantic IDs generation via residual quantization, and semantic IDs utilization for downstream retrieval and adaptation. The overall workflow is illustrated in Figure 2.

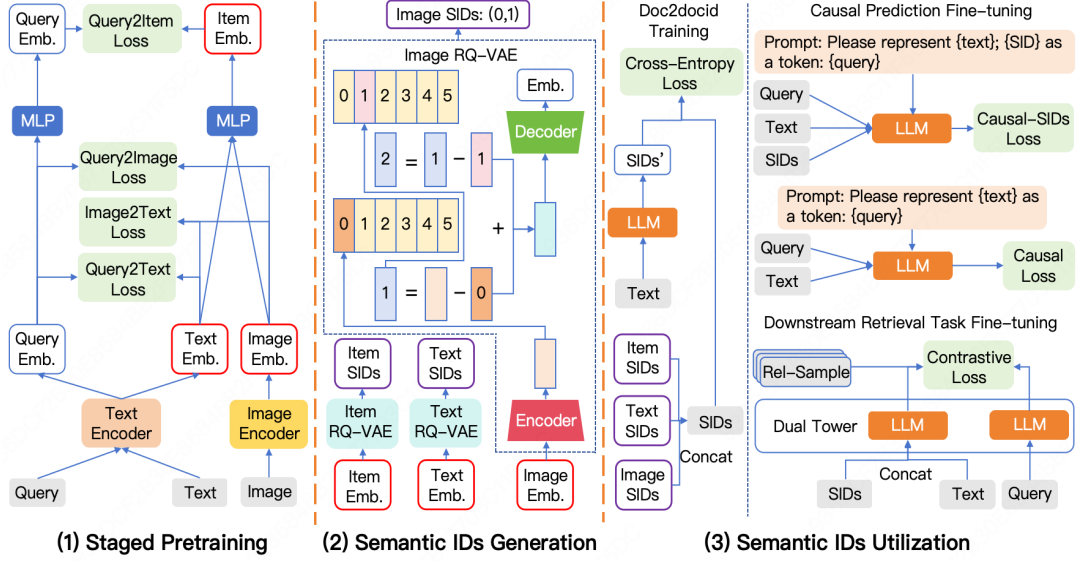


Figure 2: The overall framework of our proposed model with three principal components. 1) Staged Pretraining: High-quality multimodal embeddings are obtained through staged pretraining. 2) Semantic IDs Generation: High-dimensional embeddings are transformed into discrete SIDs to alleviate deployment burden. 3) Semantic IDs Utilization: The model is fine-tuned to adapt to SIDs, thereby enhancing downstream task performance.

4.1 Staged Pretraining

Traditional dual-tower models, which only perform contrastive learning between textual queries and items, are insufficient for real-world multimodal scenarios. In Meituan's food delivery system, the query tower typically contains only textual query features, while the item tower encompasses both textual descriptions and images of goods. Thus, we define the input as $(q, (i_{\text{text}}, i_{\text{image}}))$, where $q \in Q$ denotes the query text, $(i_{\text{text}}, i_{\text{image}}) \in \mathcal{I}$ represents the textual and image features of an item, Q is the set of queries, and \mathcal{I} is the set of items.

To reduce the multimodal gap within the item tower, we will perform contrastive learning between the textual and image features. Specifically, we pull together the representations of text and image features from the same sample and push apart those from different samples, yielding high-quality multimodal representations. This task is defined as image2text, with the loss function:

$$\mathcal{L}_{\text{image2text}} = \mathcal{L}_{\text{InfoNCE}}(h_{\text{image}}, h_{\text{text}}^+, \{h_{\text{text}}^-\}), \quad (5)$$

where negative samples are randomly sampled, $h_{\text{text}} = \text{LLM}(i_{\text{text}})$ and $h_{\text{image}} = \text{ViT}(i_{\text{image}})$, with ViT is a vision transformer used to obtain semantic embeddings from images.

In downstream retrieval tasks, although the query ultimately retrieves the fused multimodal item features, it is critical to enhance the model's understanding and responsiveness to each modality by introducing additional contrastive learning objectives between the query and various item modalities. Specifically, we define query2item, query2text, and query2image tasks, with the following

loss functions:

$$\begin{cases} \mathcal{L}_{\text{query2item}} = \mathcal{L}_{\text{InfoNCE}}(\text{MLP}_Q(h_q), \text{MLP}_I(h_{\text{item}}^+), \{\text{MLP}_I(h_{\text{item}}^-)\}), \\ \mathcal{L}_{\text{query2text}} = \mathcal{L}_{\text{InfoNCE}}(h_q, h_{\text{text}}^+, \{h_{\text{text}}^-\}), \\ \mathcal{L}_{\text{query2image}} = \mathcal{L}_{\text{InfoNCE}}(h_q, h_{\text{image}}^+, \{h_{\text{image}}^-\}), \end{cases} \quad (6)$$

where h_q , h_{text} , and h_{image} are query, text, and image embeddings encoded by the LLM, and $h_{\text{item}} = h_{\text{text}} + h_{\text{image}}$ is the fused item embedding. MLP_Q and MLP_I are projection layers for dimensionality reduction.

A common approach is joint optimization [42], where all four losses are summed for overall model training:

$$\mathcal{L}_{\text{mtrain}} = \mathcal{L}_{\text{image2text}} + \mathcal{L}_{\text{query2text}} + \mathcal{L}_{\text{query2image}} + \mathcal{L}_{\text{query2item}}. \quad (7)$$

Since joint optimization often leads to the neglect of certain modality features and the one-epoch problem, significantly compromising model performance. To address these issues, we propose a staged pretraining strategy. In the first phase, the text encoder is optimized by aligning query and text features to enhance semantic consistency. The second phase applies contrastive learning between image and text features, strengthening multimodal representations in the item tower. The third phase focuses on aligning queries with image features to improve the query tower's understanding of visual information. Finally, end-to-end optimization is performed for query-item matching to maximize retrieval performance.

This staged training strategy enables progressive optimization from simple to complex objectives, ensures focused learning at each stage, and effectively alleviates the one-epoch problem, thereby significantly enhancing the overall performance of multimodal retrieval models.

4.2 Semantic IDs Generation

After staged pretraining, we obtain high-quality multimodal embeddings and their corresponding pretrained encoders. However, resource constraints in online deployment environments make it challenging to directly utilize multimodal embeddings and to fine-tune multimodal models. To address these issues, we draw inspiration from RQ-VAE [19] techniques in generative recommendation systems. We encode multimodal feature embeddings into SIDs that retain semantic information and concatenate them as side information to the item tower's text features for downstream fine-tuning. This approach not only significantly reduces storage, computation, and inference burdens, but also enhances the text encoder's understanding and utilization of multimodal features. More details of RQ-VAE are provided in Appendix A.

We construct three independent three-layer RQ-VAE codebooks for text, image, and fused modalities, denoted as C_{text} , C_{image} , and C_{item} , respectively. The encoding process for each modality can be uniformly represented as

$$g_*(i_*) = f_{\text{RQ-VAE}}(h_*) = [\text{SIDs}_*^1, \text{SIDs}_*^2, \text{SIDs}_*^3], \quad (8)$$

where $*$ stands for text, image, or item. Here, h_* denotes the high-dimensional embedding of the corresponding modality, and $f_{\text{RQ-VAE}}(\cdot)$ represents the RQ-VAE encoding function. SIDs_*^k is the discrete semantic identifier produced by the k -th layer codebook for the corresponding modality. This hierarchical residual quantization compresses high-dimensional embeddings into compact and semantically meaningful discrete sequences, facilitating efficient indexing and retrieval.

During practical deployment, the SIDs from the fused, image, and text modalities are concatenated with the item's textual features for the item tower's text encoder, enabling embedding and downstream retrieval fine-tuning. This design not only preserves the semantic information of multimodal features, but also effectively reduces the system burden of storage, computation, and inference, and alleviates performance degradation caused by feature distribution shift. We uniformly define the *SIDs* as:

$$\text{SIDs} = [g_{\text{text}}(i_{\text{text}}), g_{\text{image}}(i_{\text{image}}), g_{\text{item}}(i_{\text{item}})]. \quad (9)$$

The final item embedding can be concisely expressed as:

$$h_i = \text{MLP}_T(\text{LLM}(\text{concat}(i_{\text{text}}, \text{SIDs}))), \quad (10)$$

where $\text{concat}(\cdot)$ denotes the operation of merging these multimodal features into a unified input.

4.3 Semantic IDs Utilization

Now we have replaced high-dimensional embeddings with SIDs as side information, effectively alleviating storage and inference burdens. However, the model still faces challenges in understanding and utilizing the newly introduced SIDs features. To address this issue, we design a series of targeted tasks, detailed as follows:

Doc2docid Training. The newly introduced SIDs, as special tokens, are not present in the original vocabulary of the LLM, making it difficult for the model to directly capture their semantic meaning. Thus, we expand the LLM's vocabulary to include all SIDs and design a supervised task to enhance its understanding. Specifically, given textual features, the model is required to predict SIDs for three modalities, enabling the LLM to learn the mapping between

text and SIDs. This task not only helps the LLM comprehend the actual semantics represented by the SIDs, but also strengthens the semantic association between SIDs and textual features, thereby improving the quality of item-side feature embeddings and retrieval performance. The loss function is defined as:

$$\mathcal{L}_{\text{doc2docid}} = \mathbb{E}_{(i_{\text{text}}, \text{SIDs})} [\text{CrossEntropy}(\text{LLM}(i_{\text{text}}), \text{SIDs})], \quad (11)$$

where $\text{CrossEntropy}(\cdot, \cdot)$ denotes the cross-entropy loss, which measures the accuracy of the LLM's SIDs prediction and encourages semantic alignment between SIDs and text.

Causal Prediction Fine-tuning. To further enhance the model's ability to capture associations between item-side and query-side features, we design a causal prediction fine-tuning task, where the model predicts the next token based on the previous context. Considering that SIDs are newly introduced features and the LLM has limited prior understanding of them, directly fine-tuning with SIDs can be challenging. Therefore, we also design an auxiliary task without SIDs to facilitate the learning process. The specific loss functions are defined as follows:

$$\begin{cases} \mathcal{L}_{\text{causal}} = \mathbb{E}_{(i_{\text{text}}, q)} \left[-\sum_{t=1}^{T-1} \log P(q_{t+1} | i_{\text{text}}, q_{1:t}) \right], \\ \mathcal{L}_{\text{causal_SIDs}} = \mathbb{E}_{(i_{\text{text}}, \text{SIDs}, q)} \left[-\sum_{t=1}^{T-1} \log P(q_{t+1} | i_{\text{text}}, \text{SIDs}, q_{1:t}) \right], \end{cases} \quad (12)$$

where T denotes the length of the query sequence, t is the current time step, and $P(q_{t+1} | \cdot)$ represents the probability that the model predicts the next query token in a causal manner given the previous context. $\mathcal{L}_{\text{causal}}$ performs causal prediction based only on item textual features, while $\mathcal{L}_{\text{causal_SIDs}}$ incorporates both item textual features and SIDs.

Downstream Retrieval Task Fine-tuning: For the downstream query-to-item retrieval task, we employ the loss function $\mathcal{L}_{\text{query2item}}$ to fine-tune the model via contrastive learning, thereby enhancing its ability to capture associations between dual-tower features. In addition to random negative sampling, we further introduce more challenging negative samples. Specifically, after the retrieval stage, the online framework utilizes a relevance model to filter candidate items; among these, some items are highly relevant to the query but were not actually clicked by the user. Such items contain implicit user preference information and are more difficult for the model to learn. By combining random negative sampling with the mining of more challenging negatives, we derive two contrastive learning loss functions to optimize the model's downstream retrieval performance.

In this component, we focus on the newly introduced SIDs features. We first employ doc2docid training to facilitate the model's understanding of these features. Subsequently, the model is further optimized using a combined loss from causal prediction fine-tuning and downstream retrieval task fine-tuning. This training strategy enables the model to establish and strengthen associations between query and item features, while also deepening its understanding of the SIDs features, thereby significantly enhancing its representational capacity and retrieval performance in retrieval tasks.

Table 1: Performance (%) comparison across different query types and datasets. R@K and N@K denote Recall@K and NDCG@K, respectively. * indicates statistically significant improvements (t-test, $p < 0.05$) over the best baseline.

| Query Type | Model | MT-Popular Cities | | | | | | MT-Other Cities | | | | | |
|-------------|------------------|-------------------|---------------|---------------|---------------|---------------|---------------|-----------------|---------------|---------------|---------------|---------------|---------------|
| | | R@5 | N@5 | R@10 | N@10 | R@20 | N@20 | R@5 | N@5 | R@10 | N@10 | R@20 | N@20 |
| All Queries | Qwen3-DualTower | 53.48 | 36.98 | 68.99 | 40.17 | 80.46 | 45.34 | 55.77 | 39.32 | 70.35 | 44.07 | 81.98 | 47.77 |
| | Joint-Que2search | 53.78 | 37.22 | 69.46 | 40.26 | 80.73 | 45.41 | 55.89 | 39.45 | 70.42 | 44.17 | 82.04 | 47.82 |
| | TIGER | 53.82 | 37.30 | 69.49 | 40.31 | 80.74 | 45.45 | 55.97 | 39.51 | 70.49 | 44.22 | 82.11 | 47.87 |
| | MTIGER | 56.01 | 39.58 | 71.18 | 42.08 | 82.42 | 47.17 | 57.95 | 41.53 | 72.44 | 46.45 | 83.56 | 49.98 |
| | SMGR | 58.19* | 41.65* | 72.92* | 44.02* | 84.10* | 48.16* | 60.10* | 43.59* | 74.50* | 48.23* | 85.48* | 51.02* |
| High-Freq | Qwen3-DualTower | 44.68 | 30.27 | 61.15 | 34.38 | 75.74 | 39.81 | 47.23 | 32.34 | 63.78 | 36.93 | 77.46 | 42.44 |
| | Joint-Que2search | 45.05 | 30.66 | 61.50 | 34.52 | 75.87 | 39.91 | 47.68 | 32.67 | 63.93 | 37.04 | 77.54 | 42.58 |
| | TIGER | 45.38 | 31.02 | 61.79 | 34.88 | 75.99 | 40.14 | 47.87 | 32.85 | 64.04 | 37.18 | 77.65 | 42.67 |
| | MTIGER | 47.91 | 32.98 | 63.68 | 36.45 | 77.58 | 41.20 | 50.05 | 35.04 | 66.36 | 39.52 | 78.92 | 44.28 |
| | SMGR | 51.12* | 35.09* | 66.74* | 38.42* | 79.50* | 42.39* | 53.42* | 37.13* | 69.49* | 41.44* | 80.78* | 45.91* |

5 Experiments

We conduct extensive experiments to answer the following research questions (RQs): **RQ1**: How does SMGR perform compared to state-of-the-art vector retrieval baselines? **RQ2**: How does staged pretraining contribute to the quality of image encoder embeddings? **RQ3**: How does the use of SIDs improve the utilization and representation of multimodal features? **RQ4**: How important is the adaptation of SIDs to downstream tasks for overall model effectiveness? **RQ5**: How does SMGR perform in real-world online retrieval scenario with industry-standard metrics? **RQ6**: How do case examples illustrate the advantages of SMGR over the baseline in real-world scenarios?

5.1 Experimental Setup

Datasets. We construct our experimental dataset using real-world data from the Meituan platform, one of the largest food delivery platforms in China. Specifically, user interaction and item data spanning one week are selected for training and validation, comprising approximately 32 million samples. Each sample includes dish ID (SPU_id), dish name (SPU_name), restaurant name (POI_name), item keywords (keywords), region information (geo_hash), and multimodal semantic IDs (item_SID, image_SID, text_SID) generated by our method. To better adapt the model to real-world user preferences, we collect hard negative samples for each query, defined as items deemed highly relevant by our relevance model but not actually selected by users; these hard negatives possess the same feature structure as the standard training samples.

For evaluation, we use real click records from the subsequent two days and partition the evaluation set by city popularity into *MT-Popular Cities* (e.g., Beijing, Shanghai, Guangzhou) and *MT-Other Cities*. Each evaluation set contains a candidate pool of 5.8 million items and 2 million user clicks. To further assess performance under more challenging conditions, we construct high-frequency subsets by selecting queries with frequency greater than 100 from both partitions.

Baselines. To comprehensively assess the effectiveness of our proposed framework, we conduct comparative experiments with several strong baseline methods across various datasets:

- **Qwen3-DualTower**: A dual-tower retrieval model based on the Facebook EBR architecture [10], where the query and item encoders are replaced with full Qwen3 [33] models as text encoders, providing robust feature encoding, instruction-following, and side information modeling capabilities.
- **Joint-Que2search**: This method employs joint training optimization within the Que2search framework [16], obtaining image embeddings through joint training and fusing them with text embeddings via an MLP for subsequent retrieval.
- **TIGER**: Utilizes RQ-VAE [19] technology to encode text embeddings into textual SIDs, which are then used alongside textual features for retrieval.
- **MTIGER**: Follows the TIGER paradigm by quantizing text, image, and fused multimodal embeddings into SIDs, concatenating them with item-side textual features, and subsequently embedding them for retrieval.

Implementation Details. For fair and consistent evaluation, all experiments use Qwen3-0.6B [33] as the text encoder and c-CLIP-ViT-h-14 [34] as the image encoder. We use three-layer MLPs to project features from 1024 to 128 dimensions for efficient deployment. Codebooks are initialized via K-means and trained with RQ-VAE, each with three quantization layers. The hidden layers adopt a pyramidal structure: [1024, 768, 512, 256] for text/image and [128, 64, 32] for multimodal features. Experiments are conducted on eight NVIDIA A100 GPUs (80GB each). The batch size is 8 for staged pretraining and 16 for downstream fine-tuning (with gradient accumulation step 8). The contrastive learning temperature is fixed at 0.05. Additional hyperparameter details are provided in the Appendix B.

Evaluation Metrics. For retrieval evaluation, FAISS [4] is employed for efficient ANN search and regional constraints are applied via *geo_hash*. Recall@K and NDCG@K ($K \in \{5, 10, 20\}$) are used as primary metrics. Each experiment is repeated ten times, and statistical significance is assessed using a paired t-test; results with $p < 0.05$ are marked with *. More details of evaluation protocol are provided in Appendix C.

5.2 Main Results (RQ1)

As shown in Table 1, our method consistently outperforms all baseline methods on both datasets. Compared with the best baseline, MTIGER, our method achieves average improvements of 3.80%, 2.64%, and 2.17% on the R@5, R@10, and R@20 metrics, respectively, and average improvements of 5.10%, 4.22%, and 2.09% on the N@5, N@10, and N@20 metrics, respectively. Furthermore, on the dataset composed of high-frequency queries, the increased number of candidate samples raises the difficulty of the retrieval task, leading to decreases in R@K and N@K metrics for all methods. Nevertheless, our method still maintains optimal performance, with average improvements over MTIGER of 6.70%, 4.81%, and 2.47% on R@5, R@10, and R@20, and 6.40%, 5.40%, and 2.89% on N@5, N@10, and N@20, respectively. These improvements are greater than those observed on the complete dataset, indicating that our method can consistently achieve superior performance even in more challenging scenarios, and the improvements are more pronounced, allowing for better adaptation to complex tasks.

We also observe that the Joint-Que2search model, which directly utilizes multimodal embeddings for retrieval, achieves performance comparable to the Qwen3-DualTower model that does not incorporate multimodal features, and performs worse than the TIGER model, which transforms text embeddings into textual SIDs. In contrast, methods that leverage multimodal SIDs, such as MTIGER and SMGR, demonstrate significantly superior performance. These results highlight the necessity of not only incorporating multimodal features but also transforming them into SIDs for effective retrieval.

Table 2: Performance (%) comparison of different multimodal feature learning methods. “Joint” refers to the model variant utilizing jointly trained image embeddings, while “Random” denotes the variant with randomly generated image embeddings. “Order” represents model variants employing staged training for image embedding generation, which are further divided into six types based on the training order; among them, “Order6” corresponds to the training sequence adopted in our proposed method. “*” indicates statistically significant improvements (t-test, $p < 0.05$) over the best variant. Further details are provided in Appendix D.

| Dataset | Variant | R@5 | N@5 | R@10 | N@10 | R@20 | N@20 |
|-------------------|---------------|---------------|---------------|---------------|---------------|---------------|---------------|
| MT-Popular Cities | Joint | 54.28 | 37.68 | 70.01 | 40.70 | 81.24 | 45.73 |
| | Random | 54.24 | 37.66 | 70.05 | 40.72 | 81.19 | 45.70 |
| | Order1 | 54.38 | 37.79 | 70.17 | 40.81 | 81.29 | 45.77 |
| | Order2 | 54.63 | 38.06 | 70.32 | 40.99 | 81.50 | 46.02 |
| | Order3 | 54.67 | 38.12 | 70.35 | 41.03 | 81.51 | 46.07 |
| | Order4 | 54.76 | 38.27 | 70.40 | 41.19 | 81.60 | 46.27 |
| | Order5 | 54.82 | 38.32 | 70.45 | 41.25 | 81.69 | 46.32 |
| MT-Other Cities | Order6 (ours) | 54.92* | 38.45* | 70.52* | 41.37* | 81.77* | 46.48* |
| | Joint | 56.28 | 39.91 | 70.79 | 44.62 | 82.34 | 48.21 |
| | Random | 56.22 | 39.86 | 70.71 | 44.56 | 82.29 | 48.17 |
| | Order1 | 56.36 | 39.99 | 70.82 | 44.66 | 82.38 | 48.27 |
| | Order2 | 56.53 | 40.19 | 70.96 | 44.87 | 82.55 | 48.47 |
| | Order3 | 56.58 | 40.23 | 70.99 | 44.89 | 82.56 | 48.50 |
| | Order4 | 56.66 | 40.28 | 71.07 | 44.92 | 82.59 | 48.60 |
| | Order5 | 56.71 | 40.37 | 71.11 | 45.02 | 82.62 | 48.67 |
| | Order6 (ours) | 56.84* | 40.49* | 71.23* | 45.13* | 82.73* | 48.81* |

5.3 Training Strategies (RQ2)

As shown in Table 2, the “Joint” variant achieves performance that is nearly identical to the “Random” variant, indicating that the model trained with joint optimization essentially ignores image features and fails to effectively utilize visual information. In contrast, our proposed method achieves consistent improvements on both datasets, with average gains of 1.09%, 0.68%, and 0.56% on R@5, R@10, and R@20, and 1.75%, 1.39%, and 1.44% on N@5, N@10, and N@20, respectively, significantly outperforming the “Joint” variant. These results indicate that staged pretraining can effectively mitigate the underutilization of image features, thereby enhancing the overall performance of the model.

Furthermore, we conduct ablation studies on the order of staged pretraining. Our approach consistently achieves the best performance across both datasets, with average improvements of 0.21%, 0.13%, and 0.12% on R@5, R@10, and R@20, and 0.32%, 0.27%, and 0.32% on N@5, N@10, and N@20, respectively, compared to the next best order (“Order5”). Additionally, in inter-tower contrastive learning, a design from easier to more difficult tasks proves to be necessary. Specifically, learning query2text before query2image effectively improves model performance (as evidenced by “Order5” outperforming “Order4”, “Order3” outperforming “Order2”, and “Order6” outperforming “Order1”). Notably, all staged pretraining variants outperform the “Joint” variant regardless of the training order, further confirming the necessity and effectiveness of the staged pretraining strategy.

Table 3: Performance (%) comparison of different multimodal feature utilization methods. Specifically, item-only, image-text, item-image, and item-text refer to variants that utilize only the SIDs corresponding to the respective modality. * indicates statistically significant improvements (t-test, $p < 0.05$) over the best variant.

| Dataset | Variant | R@5 | N@5 | R@10 | N@10 | R@20 | N@20 |
|-------------------|------------|---------------|---------------|---------------|---------------|---------------|---------------|
| MT-Popular Cities | Order6 | 54.92 | 38.45 | 70.52 | 41.37 | 81.77 | 46.48 |
| | item-only | 55.98 | 39.41 | 71.21 | 42.03 | 82.37 | 46.97 |
| | image-text | 56.52 | 39.98 | 71.70 | 42.42 | 82.78 | 47.21 |
| | item-text | 57.29 | 40.76 | 72.27 | 43.13 | 83.25 | 47.66 |
| | item-image | 57.59 | 40.99 | 72.39 | 43.35 | 83.49 | 47.88 |
| | SMGR | 58.19* | 41.65* | 72.92* | 44.02* | 84.10* | 48.16* |
| MT-Other Cities | Order6 | 56.84 | 40.49 | 71.23 | 45.13 | 82.73 | 48.81 |
| | item-only | 57.78 | 41.36 | 72.07 | 46.01 | 83.56 | 49.34 |
| | image-text | 58.34 | 41.92 | 72.71 | 46.63 | 84.08 | 49.81 |
| | item-text | 59.19 | 42.69 | 73.42 | 47.32 | 84.78 | 50.36 |
| | item-image | 59.43 | 42.83 | 73.74 | 47.56 | 84.94 | 50.48 |
| | SMGR | 60.10* | 43.59* | 74.50* | 48.23* | 85.48* | 51.02* |

5.4 Utilization of Multimodal Features (RQ3)

We conduct comparative experiments to investigate whether directly using image embeddings or converting them into SIDs and incorporating them as side information for item features would yield better performance. As shown in Table 3, compared to “Order6”, which directly uses image embeddings, our method achieves average improvements of 5.84%, 3.99%, and 3.09% on R@5, R@10, and R@20, and 7.99%, 6.64%, and 4.07% on N@5, N@10, and N@20 across both datasets.

Additionally, we perform ablation studies on the SIDs used. The results show that using only the item SIDs yields the worst performance, mainly because the compressed information it contains is insufficient to support inference. Similarly, the image-text method lacks the associative information provided by item SID, resulting in degraded model performance. Although item-image and item-text methods achieve relatively good results, their performance is suboptimal due to the absence of SIDs information from the other modality. Notably, all these methods outperform the approach of directly using image embeddings, demonstrating the necessity of converting features into SIDs before use. Moreover, the results indicate that jointly utilizing all SIDs is essential for achieving optimal performance.

5.5 Adaptation to Downstream Tasks (RQ4)

SIDs are difficult to apply directly and require appropriate fine-tuning tasks to better adapt to downstream applications. As shown in Table 4, compared to the variant that only employs a doc2docid training task, all variants that incorporate causal prediction fine-tuning achieve consistent performance improvements. Specifically, our approach achieves average improvements of 3.00%, 2.13%, and 1.73% on R@5, R@10, and R@20, and 4.16%, 3.32%, and 1.55% on N@5, N@10, and N@20 across both datasets. Furthermore, we observe that, compared to methods that use only \mathcal{L}_{causal} or $\mathcal{L}_{causal_SIDs}$, using both losses together facilitates the model's adaptation to newly introduced features, thereby achieving optimal performance.

Table 4: Performance (%) comparison of methods employing different fine-tuning tasks for downstream adaptation. * indicates statistically significant improvements (t-test, $p < 0.05$) over the best variant.

| Dataset | Variant | R@5 | N@5 | R@10 | N@10 | R@20 | N@20 |
|-------------------|--|---------------|---------------|---------------|---------------|---------------|---------------|
| MT-Popular Cities | $\mathcal{L}_{doc2docid}$ | 56.44 | 39.95 | 71.53 | 42.48 | 82.78 | 47.37 |
| | $\mathcal{L}_{doc2docid} + \mathcal{L}_{causal}$ | 57.53 | 40.92 | 72.36 | 43.44 | 83.59 | 47.87 |
| | $\mathcal{L}_{doc2docid} + \mathcal{L}_{causal_SIDs}$ | 57.33 | 40.70 | 72.18 | 43.25 | 83.37 | 47.69 |
| | SMGR | 58.19* | 41.65* | 72.92* | 44.02* | 84.10* | 48.16* |
| MT-Other Cities | $\mathcal{L}_{doc2docid}$ | 58.41 | 41.89 | 72.82 | 46.82 | 83.91 | 50.30 |
| | $\mathcal{L}_{doc2docid} + \mathcal{L}_{causal}$ | 59.37 | 42.84 | 73.79 | 47.71 | 84.80 | 50.66 |
| | $\mathcal{L}_{doc2docid} + \mathcal{L}_{causal_SIDs}$ | 59.14 | 42.61 | 73.58 | 47.51 | 84.65 | 50.48 |
| | SMGR | 60.10* | 43.59* | 74.5* | 48.23* | 85.48* | 51.02* |

5.6 Online A/B Test (RQ5)

To evaluate the real-world performance of our approach, we conduct a one-week A/B test on the Meituan platform, utilizing 10% of the total traffic. Standard industry metrics, including Revenue, CTR, Click, and cost per click (CPC), are used for assessment. All these metrics are the larger the better. As shown in Table 5, compared to the baseline Qwen3-DualTower, our method demonstrates significant improvements across all metrics. These results validate both the deployability and superior effectiveness of our approach in practical scenarios.

5.7 Case Study (RQ6)

As illustrated in Figure 3 (a), for the query "Peking Duck", the Joint-Que2search model incorrectly retrieves the item "Lotus Leaf Pancake". This error primarily arises because the POI_name feature

Table 5: Improvements in the week-long online A/B test.

| Revenue | CTR | Click | CPC |
|---------|--------|--------|--------|
| +1.12% | +1.02% | +0.72% | +0.19% |

contains the term "Roast Duck", which is semantically related to the query and leads to a false positive retrieval. This case demonstrates that the joint optimization process tends to focus predominantly on textual features while neglecting image features.

In contrast, for the same query "Peking Duck", even when neither the POI_name ("Ziguangyuan Restaurant") nor the SPU_name ("Whole Set Meal") contains features directly related to the query, the SMGR model is still able to correctly retrieve the target item by leveraging the image of "Roast Duck". This demonstrates that SMGR can effectively utilize multimodal features to enhance retrieval performance and better respond to user queries.

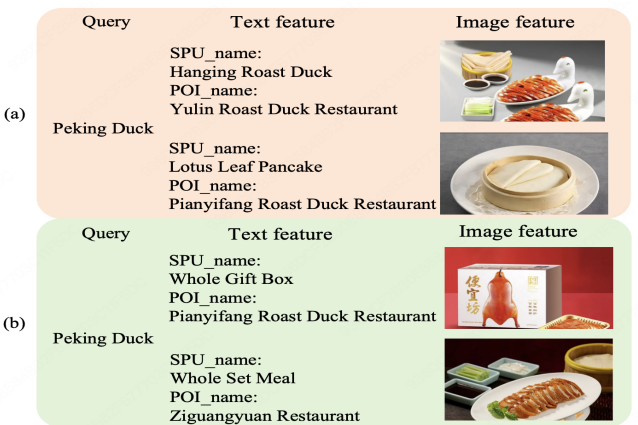


Figure 3: The Top-2 retrieved items for the query "Peking Duck" produced by different models: (a) baseline Joint-Que2search; (b) our proposed SMGR.

6 Conclusion

In this paper, we identify issues in multimodal retrieval, such as the neglect of modality features and the one-epoch problem caused by joint optimization, and proposes the SMGR method to address these challenges. The staged pretraining strategy in SMGR enables the model to focus on the specific task of each stage, thereby mitigating these problems. By converting high-dimensional embeddings into SIDs, the method alleviates resource and deployment burdens. Furthermore, by introducing both generative and discriminative SIDs understanding and adaptation tasks, our approach improves downstream retrieval performance. Extensive online and offline experiments in real-world scenarios demonstrate the effectiveness of the proposed framework. For future work, we plan to incorporate user historical information on the query side to better capture user preferences. In addition, we intend to explore the generation and utilization of SIDs for sequential data, further broadening the applicability of our approach to more diverse scenarios.

References

- [1] Mustafa Abdool, Soumyadip Banerjee, Moutupsi Paul, Do-kyum Kim, Xiaowei Liu, Bin Xu, Tracy Yu, Hui Gao, Karen Ouyang, Huiji Gao, et al. 2026. Applying Embedding-Based Retrieval to Airbnb Search. arXiv preprint arXiv:2601.06873.
- [2] Gaode Chen, Ruina Sun, Yuezhan Jiang, Jiangxia Cao, Qi Zhang, Jingjian Lin, Han Li, Kun Gai, and Xinghua Zhang. 2024. A Multi-modal Modeling Framework for Cold-start Short-video Recommendation. In *Proceedings of the 18th ACM Conference on Recommender Systems*. ACM, Bari, Italy, 391–400.
- [3] Paul Covington, Jay Adams, and Emre Sargin. 2016. Deep neural networks for youtube recommendations. In *Proceedings of the 10th ACM conference on recommender systems*. ACM, Boston, MA, USA, 191–198.
- [4] Matthijs Douze, Alexandre Guizilini, Chengqi Deng, Jeff Johnson, Gergely Szilvassy, Pierre-Emmanuel Mazaré, Maria Lomeli, Lucas Hosseini, and Hervé Jégou. 2025. The faiss library. *IEEE Transactions on Big Data* (2025), 1–17.
- [5] Kairui Fu, Tao Zhang, Shuwen Xiao, Ziyang Wang, Xinning Zhang, Chenchi Zhang, Yuliang Yan, Junjun Zheng, Yu Li, Zhihong Chen, et al. 2025. Forge: Forming semantic identifiers for generative retrieval in industrial datasets. arXiv preprint arXiv:2509.20904.
- [6] Guobing Gan, Kaiming Gao, Li Wang, Shen Jiang, and Peng Jiang. 2025. HCMRM: A High-Consistency Multimodal Relevance Model for Search Ads. In *Companion Proceedings of the ACM on Web Conference 2025*. ACM, Sydney, Australia, 201–210.
- [7] Tengyu Han, Pengfei Wang, Shaozhang Niu, and Chenliang Li. 2022. Modality matches modality: Pretraining modality-disentangled item representations for recommendation. In *Proceedings of the ACM web conference 2022*. ACM, Lyon, France, 2058–2066.
- [8] Xintian Han, Honggang Chen, Quan Lin, Jingyue Gao, Xiangyuan Ren, Lifei Zhu, Zhisheng Ye, Shikang Wu, XiongHang Xie, Xiaochu Gan, et al. 2025. LEMUR: Large scale End-to-end MUltimodal Recommendation. arXiv preprint arXiv:2511.10962.
- [9] Yi-Ping Hsu, Po-Wei Wang, Chantat Eksombatchai, and Jiajing Xu. 2024. Taming the One-Epoch Phenomenon in Online Recommendation System by Two-stage Contrastive ID Pre-training. In *Proceedings of the 18th ACM Conference on Recommender Systems*. ACM, Bari, Italy, 838–840.
- [10] Jui-Ting Huang, Ashish Sharma, Shuying Sun, Li Xia, David Zhang, Philip Pronin, Janani Padmanabhan, Giuseppe Ottaviano, and Linjun Yang. 2020. Embedding-based retrieval in facebook search. In *Proceedings of the 26th ACM SIGKDD International Conference on Knowledge Discovery & Data Mining*. ACM, San Diego, CA, USA, 2553–2561.
- [11] Po-Sen Huang, Xiaodong He, Jianfeng Gao, Li Deng, Alex Acero, and Larry Heck. 2013. Learning deep structured semantic models for web search using clickthrough data. In *Proceedings of the 22nd ACM international conference on Information & Knowledge Management*. ACM, San Francisco, CA, USA, 2333–2338.
- [12] Weitao Jia, Shuo Yin, Zhoufutu Wen, Han Wang, Zehui Dai, Kun Zhang, Zhenyu Li, Tao Zeng, and Xiaohui Lv. 2025. SUMMA: A Multimodal Large Language Model for Advertisement Summarization. In *Proceedings of the 34th ACM International Conference on Information and Knowledge Management*. ACM, Seoul, Korea, 1156–1167.
- [13] Omar Khattab and Matei Zaharia. 2020. Colbert: Efficient and effective passage search via contextualized late interaction over bert. In *Proceedings of the 43rd International ACM SIGIR conference on research and development in Information Retrieval*. ACM, Virtual Event, 39–48.
- [14] Junnan Li, Ramprasaath Selvaraju, Akhilesh Gotmare, Shafiq Joty, Caiming Xiong, and Steven Chu Hong Hoi. 2021. Align before fuse: Vision and language representation learning with momentum distillation. *Advances in neural information processing systems* 34 (2021), 9694–9705.
- [15] Zida Liang, Changfu Wu, Dunxian Huang, Weiqiang Sun, Ziyang Wang, Yuliang Yan, Jian Wu, Yunjing Jiang, Bo Zheng, Ke Chen, et al. 2025. Tbgrecall: A generative retrieval model for e-commerce recommendation scenarios. In *Proceedings of the 34th ACM International Conference on Information and Knowledge Management*. ACM, Seoul, Korea, 5863–5870.
- [16] Yiqun Liu, Kaushik Rangadurai, Yunzhong He, Siddarth Malreddy, Xunlong Gui, Xiaoyi Liu, and Fedor Borisyuk. 2021. Que2search: fast and accurate query and document understanding for search at facebook. In *Proceedings of the 27th ACM SIGKDD Conference on Knowledge Discovery & Data Mining*. ACM, Singapore, 3376–3384.
- [17] Yifan Liu, Kangning Zhang, Xiangyuan Ren, Yanhua Huang, Jiarui Jin, Yingjie Qin, Rui long Su, Ruiwen Xu, Yong Yu, and Weinan Zhang. 2024. Alignrec: Aligning and training in multimodal recommendations. In *Proceedings of the 33rd ACM International Conference on Information and Knowledge Management*. ACM, Boise, ID, USA, 1503–1512.
- [18] Xincheng Luo, Jiangxia Cao, Tianyu Sun, Jinkai Yu, Rui Huang, Wei Yuan, Hezheng Lin, Yichen Zheng, Shiyao Wang, Qigen Hu, et al. 2025. Qarm: Quantitative alignment multi-modal recommendation at kuaishou. In *Proceedings of the 34th ACM International Conference on Information and Knowledge Management*. ACM, Seoul, Korea, 5915–5922.
- [19] Shashank Rajput, Nikhil Mehta, Anima Singh, Raghunandan Hulikal Keshavan, Trung Vu, Lukasz Heldt, Lichan Hong, Yi Tay, Vinh Tran, Jonah Samost, et al. 2023. Recommender systems with generative retrieval. *Advances in Neural Information Processing Systems* 36 (2023), 10299–10315.
- [20] Nils Reimers and Iryna Gurevych. 2019. Sentence-BERT: Sentence Embeddings using Siamese BERT-Networks. In *Proceedings of the 2019 Conference on Empirical Methods in Natural Language Processing and the 9th International Joint Conference on Natural Language Processing*. ACL, Hong Kong, PRC, 3982–3992.
- [21] Yelong Shen, Xiaodong He, Jianfeng Gao, Li Deng, and Grégoire Mesnil. 2014. A latent semantic model with convolutional-pooling structure for information retrieval. In *Proceedings of the 23rd ACM international conference on conference on information and knowledge management*. ACM, Shanghai, PRC, 101–110.
- [22] Yelong Shen, Xiaodong He, Jianfeng Gao, Li Deng, and Grégoire Mesnil. 2014. Learning semantic representations using convolutional neural networks for web search. In *Proceedings of the 23rd international conference on world wide web*. ACM, Seoul, Korea, 373–374.
- [23] Xiang-Rong Sheng, Feifei Yang, Litong Gong, Biao Wang, Zhangming Chan, Yujing Zhang, Yueyao Cheng, Yong-Nan Zhu, Tiezheng Ge, Han Zhu, et al. 2024. Enhancing Taobao Display Advertising with Multimodal Representations: Challenges, Approaches and Insights. In *Proceedings of the 33rd ACM International Conference on Information and Knowledge Management*. ACM, Boise, ID, USA, 4858–4865.
- [24] Weiwei Sun, Lingyong Yan, Zheng Chen, Shuaiqiang Wang, Haichao Zhu, Pengjie Ren, Zhumin Chen, Dawei Yin, Maarten Rijke, and Zhaochun Ren. 2023. Learning to tokenize for generative retrieval. *Advances in Neural Information Processing Systems* 36 (2023), 46345–46361.
- [25] Hongwei Wang, Fuzheng Zhang, Xing Xie, and Minyi Guo. 2018. DKN: Deep knowledge-aware network for news recommendation. In *Proceedings of the 2018 world wide web conference*. ACM, Lyon, France, 1835–1844.
- [26] Shijia Wang, Tianpei Ouyang, Qiang Xiao, Dongjing Wang, Yintao Ren, Songpei Xu, Da Guo, and Chuanjiang Luo. 2025. Progressive Semantic Residual Quantization for Multimodal-Joint Interest Modeling in Music Recommendation. In *Proceedings of the 34th ACM International Conference on Information and Knowledge Management*. ACM, Seoul, Korea, 6119–6127.
- [27] Bin Wu, Feifei Yang, Zhangming Chan, Yu-Ran Gu, Jiawei Feng, Chao Yi, Xiang-Rong Sheng, Han Zhu, Jian Xu, Mang Ye, et al. 2025. MUSE: A Simple Yet Effective Multimodal Search-Based Framework for Lifelong User Interest Modeling. arXiv preprint arXiv:2512.07216.
- [28] Chuhan Wu, Fangzhao Wu, Mingxiao An, Jianqiang Huang, Yongfeng Huang, and Xing Xie. 2019. NPA: neural news recommendation with personalized attention. In *Proceedings of the 25th ACM SIGKDD international conference on knowledge discovery & data mining*. ACM, Anchorage, Alaska, USA, 2576–2584.
- [29] Chuhan Wu, Fangzhao Wu, Suyu Ge, Tao Qi, Yongfeng Huang, and Xing Xie. 2019. Neural news recommendation with multi-head self-attention. In *Proceedings of the 2019 conference on empirical methods in natural language processing and the 9th international joint conference on natural language processing*. ACL, Hong Kong, PRC, 6389–6394.
- [30] Yanjing Wu, Yin Feng, Jian Wang, Wenji Zhou, Yunan Ye, Rong Xiao, and Jun Xiao. 2024. Hi-gen: Generative retrieval for large-scale personalized e-commerce search. In *Proceedings of the 24th IEEE International Conference on Data Mining*. IEEE, Abu Dhabi, UAE.
- [31] Yi Xu, Moyu Zhang, Chenxuan Li, Zhihao Liao, Haibo Xing, Hao Deng, Jinxin Hu, Yu Zhang, Xiaoyi Zeng, and Jing Zhang. 2025. Mmq: Multimodal mixture-of-quantization tokenization for semantic id generation and user behavioral adaptation. arXiv preprint arXiv:2508.15281.
- [32] Bencheng Yan, Si Chen, Shichang Jia, Jianyu Liu, Yueran Liu, Chenghan Fu, Wanxian Guan, Hui Zhao, Xiang Zhang, Kai Zhang, et al. 2025. MIM: Multimodal Content Interest Modeling Paradigm for User Behavior Modeling. arXiv preprint arXiv:2502.00321.
- [33] An Yang, Anfeng Li, Baosong Yang, Beichen Zhang, Binyuan Hui, Bo Zheng, Bowen Yu, Chang Gao, Chengan Huang, Chenxu Lv, et al. 2025. Qwen3 technical report. arXiv preprint arXiv:2505.09388.
- [34] An Yang, Junshu Pan, Junyang Lin, Rui Men, Yichang Zhang, Jingren Zhou, and Chang Zhou. 2022. Chinese clip: Contrastive vision-language pretraining in chinese. arXiv preprint arXiv:2211.01335.
- [35] Wencai Ye, Mingjie Sun, Shuhang Chen, Wenjin Wu, and Peng Jiang. 2025. Align³ GR: Unified Multi-Level Alignment for LLM-based Generative Recommendation. arXiv preprint arXiv:2511.11255.
- [36] Wencai Ye, Mingjie Sun, Shaoyun Shi, Peng Wang, Wenjin Wu, and Peng Jiang. 2025. DAS: Dual-Aligned Semantic IDs Empowered Industrial Recommender System. In *Proceedings of the 34th ACM International Conference on Information and Knowledge Management*. ACM, Seoul, Korea, 6217–6224.
- [37] Peiwen Yuan, Xinglin Wang, Shaoxiong Feng, Boyuan Pan, Yiwei Li, Heda Wang, Xupeng Miao, and Kan Li. 2024. Generative Dense Retrieval: Memory Can Be a Burden. In *Proceedings of the 18th Conference of the European Chapter of the Association for Computational Linguistics (Volume 1: Long Papers)*. ACL, St. Julians, Malta, 2835–2845.

[38] Chao Zhang, Haixin Zhang, Shiwei Wu, Di Wu, Tong Xu, Xiangyu Zhao, Yan Gao, Yao Hu, and Enhong Chen. 2025. Notellm-2: Multimodal large representation models for recommendation. In *Proceedings of the 31st ACM SIGKDD Conference on Knowledge Discovery and Data Mining* V. 1. ACM, Toronto, ON, Canada, 2815–2826.

[39] Hailin Zhang, Yujing Wang, Qi Chen, Ruiheng Chang, Ting Zhang, Ziming Miao, Yingyan Hou, Yang Ding, Xupeng Miao, Haonan Wang, et al. 2023. Model-enhanced vector index. *Advances in Neural Information Processing Systems* 36 (2023), 54903–54917.

[40] Zhao-Yu Zhang, Xiang-Rong Sheng, Yujing Zhang, Biye Jiang, Shuguang Han, Hongbo Deng, and Bi Zheng. 2022. Towards understanding the overfitting phenomenon of deep click-through rate models. In *Proceedings of the 31st ACM international conference on information & knowledge management*. ACM, Atlanta, GA, USA, 2671–2680.

[41] Xinpeng Zhao, Zhaochun Ren, Yukun Zhao, Zhenyang Li, Mengqi Zhang, Jun Feng, Ran Chen, Ying Zhou, Zhumin Chen, Shuaiciqiang Wang, et al. 2025. DiffuGR: Generative Document Retrieval with Diffusion Language Models. arXiv preprint arXiv:2511.08150.

[42] Zhigong Zhou, Ning Ding, Xiaochuan Fan, Yue Shang, Yiming Qiu, Jingwei Zhuo, Zhiwei Ge, Songlin Wang, Lin Liu, Sulong Xu, et al. 2023. Semantic-enhanced modality-asymmetric retrieval for online e-commerce search. In *Proceedings of the 46th International ACM SIGIR Conference on Research and Development in Information Retrieval*. ACM, Taipei, Taiwan, 3405–3409.

A Details of RQ-VAE

RQ-VAE is a generative model designed to compress high-dimensional continuous embeddings into compact and semantically meaningful discrete representations via multi-layer residual quantization. At each quantization layer l , the process is defined as:

$$e^{(l)} = \text{Quantize}^{(l)}(r^{(l)}), \quad r^{(1)} = h, \quad r^{(l+1)} = r^{(l)} - e^{(l)}, \quad (13)$$

where h denotes the high-dimensional input embedding, $\text{Quantize}^{(l)}(\cdot)$ denotes the nearest neighbor lookup in the l -th codebook, and L is the number of quantization layers. The final discrete semantic representation is formed by concatenating the codebook indices from each layer, $[c^{(1)}, c^{(2)}, \dots, c^{(L)}]$, which serves as the SIDs and is used as side information in subsequent item tower features.

During RQ-VAE training, the loss function incorporates three components: reconstruction loss, codebook loss, and commitment loss. For an input embedding h and its reconstruction \hat{h} , the total loss is given by:

$$\mathcal{L}_{\text{RQ-VAE}} = \|h - \hat{h}\|_2^2 + \beta \sum_{l=1}^L \left(\|\text{sg}[r^{(l)}] - e^{(l)}\|_2^2 + \gamma \|r^{(l)} - \text{sg}[e^{(l)}]\|_2^2 \right) \quad (14)$$

where the first term, $\|h - \hat{h}\|_2^2$, is the reconstruction loss, measuring how well the encoded discrete SIDs can recover the original embedding and ensuring semantic integrity. The second term, $\|\text{sg}[r^{(l)}] - e^{(l)}\|_2^2$, is the codebook loss, encouraging the encoder outputs to approximate the discrete vectors in the quantization codebook. The third term, $\|r^{(l)} - \text{sg}[e^{(l)}]\|_2^2$, is the commitment loss, which constrains the encoder outputs to adapt to the codebook, promoting collaborative updates between the codebook and feature distribution. Here, $\text{sg}[\cdot]$ denotes the stop-gradient operator, and β , γ are hyperparameters balancing the loss terms.

B Hyperparameter Settings

To ensure consistency in training and evaluation, we employ Qwen3-0.6B as the text encoder for both query and item textual features in all experiments, and utilize a staged pretraining cn-CLIP-ViT-h-14 as the image encoder for item images. Prior to RQ-VAE training, codebooks are initialized using K-means, followed by independent

three-layer codebook training for item, image, and text embeddings, with each layer containing 32 entries and no parameter sharing. The item codebook uses 128-dimensional input/output with three hidden layers [128, 64, 32], while the image and text codebooks use 1024-dimensional input/output with four hidden layers [1024, 768, 512, 256]. The commitment loss weight β and codebook update loss weight γ are both set to 0.25, with candidate values in [0.05, 0.1, 0.15, 0.2, 0.25, 0.3, 0.35, 0.4, 0.45, 0.5].

All experiments are conducted on eight Nvidia A100 GPUs (80GB each), with memory usage ranging from 100GB to 800GB depending on task requirements. The batch size is set to 8 during staged pretraining and 16 during downstream fine-tuning, with gradient accumulation every 8 steps. The temperature for contrastive learning is set to 0.05, with candidate values in [0.01, 0.02, 0.03, 0.04, 0.05, 0.06, 0.07, 0.08, 0.09, 0.1].

C Evaluation Protocol

For evaluation, both candidate items and queries from the click logs are embedded separately, and FAISS is used to partition the search space to accelerate recall computation. Notably, for a given geo_hash, queries are only matched with candidate items from the same geo_hash, reflecting real user behavior. To ensure the reliability of experimental results, each experiment is repeated ten times. A paired t-test is performed to assess the statistical significance of performance differences between models. Results with $p < 0.05$ are considered statistically significant improvements and are marked with * in the tables. Recall@K and NDCG@K are reported as the main evaluation metrics, where $K \in \{5, 10, 20\}$.

D Ablation Variants

- **Joint**: All four losses (image2text, query2image, query2text, query2item) are summed and optimized jointly.
- **Random**: Text features are embedded using the trained Joint model's text encoder, while image features are replaced with randomly generated vectors.
- **Order1–Order6**: Different staged pretraining orders, including:
 - Order1: query2image, image2text, query2text, query2item
 - Order2: query2image, query2text, image2text, query2item
 - Order3: query2text, query2image, image2text, query2item
 - Order4: image2text, query2image, query2text, query2item
 - Order5: image2text, query2text, query2image, query2item
 - Order6: query2text, image2text, query2image, query2item
- **Item-only**: Uses only item_SIDs as item-side information.
- **Image-text**: Uses image_SIDs and text_SIDs as item-side information.
- **Item-image**: Uses image_SIDs and item_SIDs as item-side information.
- **Item-text**: Uses text_SIDs and item_SIDs as item-side information.
- **All_SIDs**: Uses image_SIDs, text_SIDs, and item_SIDs as item-side information.
- $\mathcal{L}_{\text{doc2docid}}$: Only performs SIDs prediction for trained models.
- $\mathcal{L}_{\text{doc2docid}} + \mathcal{L}_{\text{causal}}$: Performs both SIDs prediction and causal prediction fine-tuning on sentences containing item-side (without SIDs) and query-side features.

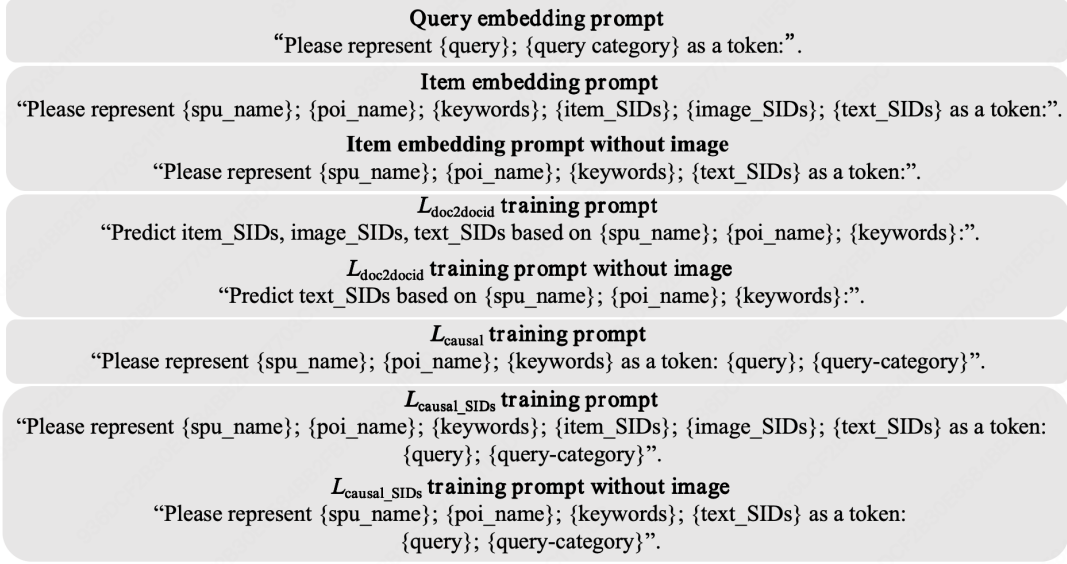


Figure 4: Examples of prompt templates used during training, fine-tuning, and inference.

- $\mathcal{L}_{\text{doc2docid}} + \mathcal{L}_{\text{causal_SIDs}}$: Performs both SIDs prediction and causal prediction fine-tuning on sentences containing item-side (with SIDs) and query-side features.

E Prompt Templates

As illustrated in Figure 4, representative examples of prompt templates utilized during model training, fine-tuning, and inference are presented.